1,1-Dichloroethane: A Molecular Crystal Structure without van der Waals Contacts?

Maciej Bujak,[†] Marcin Podsiadło,[‡] and Andrzej Katrusiak*[,‡]

Institute of Chemistry, University of Opole, Oleska 48, 45-052 Opole, Poland, and Faculty of Chemistry, Adam Mickiewicz University, Grunwaldzka 6, 60-780 Poznań, Poland

Received: July 13, 2007; In Final Form: October 15, 2007

Isochoric and isobaric freezing of 1,1-dichloroethane, CH_3CHCl_2, mp = 176.19 K, yielded the orthorhombic structure, space group *Pnma*, with the fully ordered molecules, in the staggered conformation, located on mirror planes. The CH_3CHCl_2 ambient-pressure (0.1 MPa) structures were determined at 160 and 100 K, whereas the 295 K high-pressure structures were determined at 0.59 and 1.51 GPa. At 0.1 MPa, all intermolecular distances are considerably longer than the sums of the van der Waals radii, and only a pressure of about 1.5 GPa squeezed the Cl···Cl and Cl···H contacts to distances commensurate with these sums. The exceptionally large difference between the melting points of isomeric 1,1- and 1,2-dichloroethane can be rationalized in terms of their molecular-packing efficiency. It has been shown that the location of atoms in molecules affects their intermolecular interactions, and hence their van der Waals radii are the function of molecular structures.

1. Introduction

Ethane and its halogen derivatives have been often applied as the model structures for studying conformational transformations, steric effects, molecular interactions, crystal packing, and their relations with physical and chemical properties such as phase transitions, compressibility, as well as melting temperature/freezing pressure, in an organic molecular system.[1−3] The structure−melting point relationships studied by several groups[2,4−9] were mainly concentrated on homologous subsets of organic molecules. The variations of melting points among homologous substances, isomers, and those of close stoichiometry are believed to be mainly due to different packing efficiency. Most recently we investigated these relations for dichlorobenzenes,[10] dibromobenzenes, and halogenated ethanes.

Both 1,2-dichloroethane (12DCE,[11]) and 1,1,2,2-tetrachloroethane (1122TCE,[12]) form ordered and disordered crystal phases, where the contacts between halogen atoms are clearly distinguishable in the molecular arrangement in the structures determined at low temperature and in the structures determined at high pressure. In those structures the lengths of the Cl···Cl contacts are shorter than the sums of van der Waals radii of these atoms. In 12DCE the transformation between the disordered and ordered phases has the character of isostructural transition, and the abrupt change of Cl···Cl distances suggests that the crystal structure is dominated by the Cl···Cl interactions adjusting to the required space for the rotations of ethylene groups. Thus it appeared that in this structure the internal disorder competes with the intermolecular Cl···Cl contacts. On the other hand, it can be argued that the densely packed molecules interact with each other and that their interactions are changed at the transition stage. From this point of view, the Cl···Cl contacts can be considered as a consequence of the terminal location of atoms in molecules and not caused by significant differences between the energies of the Cl···Cl and other secondary-bond interactions.[13,14]

* To whom correspondence should be addressed. E-mail: katran@amu.edu.pl.

[†] University of Opole.

[‡] Adam Mickiewicz University.

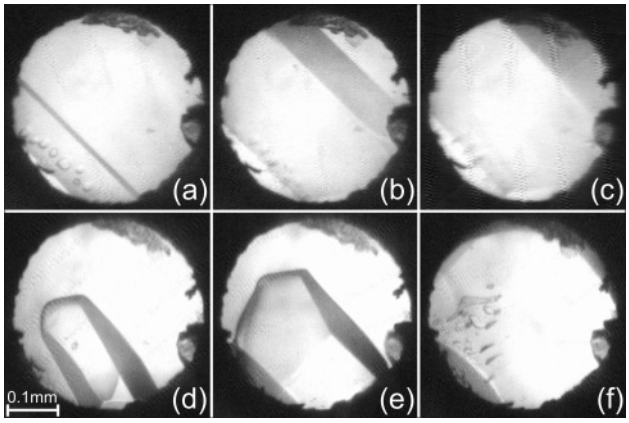

Figure 1. Single-crystal growth stages of 11DCE in a DAC at 0.59 GPa (a−c) and 1.51 GPa (d−f).

Presently we have complemented those studies by determining the structure of 1,1-dichloroethane (11DCE) crystallized by isochoric and isobaric freezing. 11DCE is the isomer of 12DCE. In this C_s-symmetric molecule, two Cl atoms are located at the same carbon atom, and therefore they are less exposed, compared to 12DCE, to intermolecular contacts. Despite numerous studies of 11DCE by nuclear magnetic resonance,[15,16] infrared, Raman,[17−19] and microwave spectroscopy,[20] neutron inelastic scattering,[21] electron diffraction,[22] and other methods,[23] the exceptional and largest among all chloroethane isomers difference in the melting points of ca. 61 K[24] between 11DCE and 12DCE has not been explained, on the molecular level.

2. Experimental Methods

2.1. In Situ Low-Temperature and High-Pressure Crystal Growth. Commercially available 11DCE (pure, Fluka AG) was used without further purification. The isobaric crystallization of 11DCE was carried out in a glass capillary with an internal diameter of 0.3 mm and 0.01 mm of wall thickness (Hilgenberg GmbH, Germany). The liquid sample filling 2−3 mm of the sealed capillary was cooled in a nitrogen gas stream, using an Oxford Cryosystems attachment of a diffractometer. Setting the

10.1021/jp075491p CCC: $40.75
Published on Web 01/09/2008

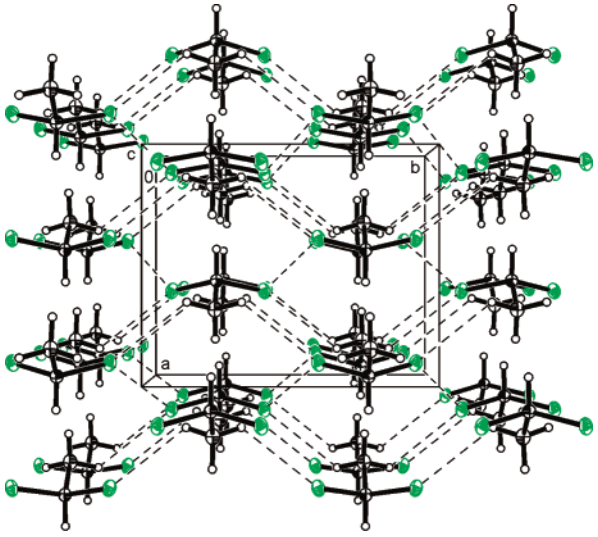

Figure 2. Crystal structure of 11DCE at 295 K and 1.51 GPa along its *c* axis. The dashed lines indicate the shortest Cl···Cl and Cl···H intermolecular contacts (Table 2). Displacement ellipsoids are plotted at the 25% probability level.

temperature of the gas stream of 110 K yielded a polycrystalline material, which was warmed up to the temperature of ca. 170 K. Growth of the single crystal was achieved by the cyclic melting and freezing of a polycrystalline material, at a rate of 1 K·min^{-1}, within the range of 174−176.5 K, allowing one small crystal seed left in each cycle, which eventually grew in all the sample volume.[25−27] The first X-ray intensity data were collected at 160 K, and the second data set for another bigger crystal was obtained in the same way but cooled down to 100 K.

The high-pressure crystallization of a single crystal of 11DCE was carried out in a modified Merrill−Bassett diamond-anvil cell, DAC.[28] A general description of this high-pressure crystallization method has already been reported.[11,29−31] The diameter of the diamond culets was 0.8 mm. The gasket was made of 0.3 mm thick steel foil with a 0.45 mm in diameter hole spark-eroded and pre-indented to 0.28 mm.[32] The freezing pressure of 0.52(5) GPa was measured, when the polycrystalline and liquid 11DCE sample coexisted in the high-pressure chamber. After nucleation the polycrystalline sample was heated with a hot-air gun until all but one crystallite melted. This seed was allowed to grow, giving a disc-shaped single crystal (parts a−c of Figure 1). The first data set was collected at 0.59(5) GPa. Then the crystal sample was almost completely melted at 460 K, the screws of the DAC were tightened, and a single crystal at 1.51(5) GPa was obtained (parts d−f of Figure 1). The pressure in a DAC was determined using a BETSA PRL spectrometer, from the ruby-fluorescence line shift[33] with the accuracy of ca. 0.05 GPa.

2.2. Data Collection, Data Reduction, and Refinement. The low-temperature/ambient-pressure and room-temperature/high-pressure diffraction data were collected on a KM-4 CCD diffractometer with the graphite-monochromated Mo Kα radiation. At 160 and 100 K, the reflections were measured using the ω-scan techniques with $\Delta\omega = 0.75°$ and 10- and 15-s exposure times, respectively. The pressure-frozen single crystals of 11DCE were centered on the diffractometer by the shadow method.[34] Intensity data were collected using the φ- and ω-scan techniques with $\Delta\omega/\Delta\varphi = 0.7°$ and 25 s exposures.

All data were accounted for by the Lorentz, polarization, and sample absorption effects[35−38] and in the case of the high-pressure measurements for the absorption of the X-rays by DAC and shadowing of the single crystal by the gasket edges.[37,38] The gasket shadowing allowed 0.49−0.98 of the sample crystal volume to efficiently scatter at 0.59(5) GPa, and 0.51−0.94 at 1.51(5) GPa. All structures were solved by direct methods and refined with SHELX-97.[39] The Cl and C atoms were refined with anisotropic displacement parameters. All hydrogen atoms were located in subsequent difference Fourier maps, refined with C−H distance constrained and U_{eq} values equal for CH_3 and CH, respectively, to 1.5 and 1.2 times the U_{eq} value of their carriers. The CrysAlis CCD and CrysAlis RED programs[35] were used for the data collection, unit-cell refinement, and data reductions (initial reduction of the high-pressure intensity data).

The analysis of intermolecular interactions was performed with the program CrystalExplorer.[40,41] In the newest version of this program, the scale intermolecular distances are referred to the van der Waals radii, which is different from the initial versions of this program, when it was first applied for the analysis of high-pressure structures.[42] The crystal structures were drawn by program XP.[36,43]

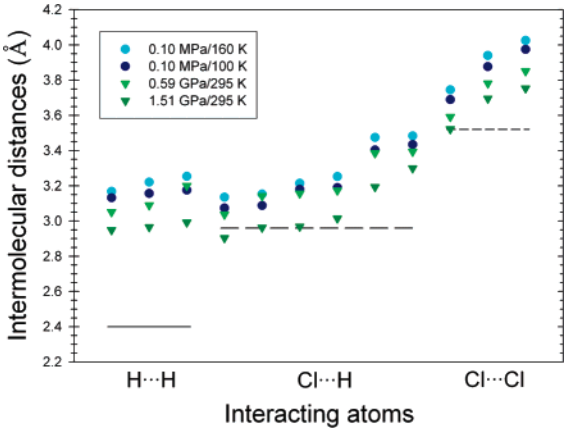

Figure 3. The evolution of the shortest H···H, Cl···H, and Cl···Cl intermolecular distances with temperature and pressure for 11DCE. The horizontal solid and dashed lines indicate the sums of van der Waals radii for relevant atoms.

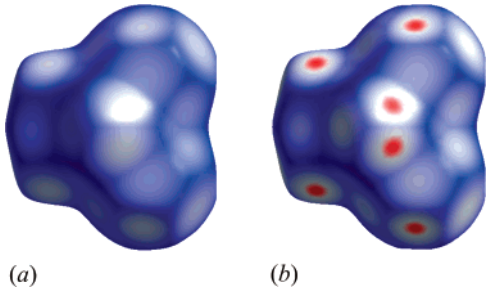

Figure 4. The Hirshfeld surface for the 11DCE molecule at (a) 160 K/0.1 MPa and (b) 295 K/1.51 GPa. The color scale describes distances longer (shades of navy-blue), equal (white), and shorter (red) than the van der Waals radii. The program CrystalExplorer[40,41] was used for preparing these drawings.

3. Results and Discussion

According to Kitajgorodskij the orthorhombic crystal of 11DCE, space group *Pnma*, with the fully ordered C_s-symmetric molecules can be classified as "limitingly close-packed".[44,45] Both its large molecular coordination number of 14,[45,46] and the packing coefficients between 0.65 and 0.77, are characteristic for organic (molecular) crystals (Figure 2).

3.1. Low-Temperature and High-Pressure Structures of 11DCE. The molecular dimensions of 11DCE are consistent with those obtained by electron diffraction[22] and microwave

TABLE 1: 11DCE Crystal Data and Structure Determination Summary

temperature pressure	100.0(1) K 0.1 MPa	160.0(1) K 0.1 MPa	295(2) K 0.59(5) GPa	295(2) K 1.51(5) GPa
formula	$C_2H_4Cl_2$	$C_2H_4Cl_2$	$C_2H_4Cl_2$	$C_2H_4Cl_2$
fw, g/mol	98.95	98.95	98.95	98.95
cryst size, mm^3	0.30 × 0.30 × 0.10	0.20 × 0.20 × 0.10	0.40 × 0.38 × 0.23	0.39 × 0.38 × 0.23
cryst syst	orthorhombic	orthorhombic	orthorhombic	orthorhombic
space group, Z	*Pnma*, 4	*Pnma*, 4	*Pnma*, 4	*Pnma*, 4
a, Å	7.7446(9)	7.8716(16)	7.5572(9)	7.3833(10)
b, Å	9.3368(10)	9.404(2)	9.1829(18)	9.0641(11)
c, Å	5.8584(7)	5.8862(11)	5.713(3)	5.6461(18)
V, $Å^3$	423.62(8)	435.71(15)	396.5(2)	377.86(14)
ρ, g/cm^3	1.552	1.508	1.658	1.739
μ, mm^{-1}	1.304	1.268	1.394	1.462
θ range, °	3.41−29.66	3.46−29.12	2.69−29.18	2.76−29.33
index ranges	$-9 \le h \le 9$ $-11 \le k \le 10$ $-6 \le l \le 7$	$-9 \le h \le 6$ $-9 \le k \le 11$ $-6 \le l \le 7$	$-9 \le h \le 9$ $-10 \le k \le 10$ $-4 \le l \le 4$	$-8 \le h \le 8$ $-10 \le k \le 10$ $-4 \le l \le 4$
reflns coll	2552	1983	2372	2383
R_{int}	0.0458	0.1073	0.0626	0.0808
data [$I > 2\sigma(I)$]	404	407	180	244
data/parameters	406/30	417/30	183/29	253/29
GOF on F^2	1.238	1.249	1.197	1.106
R_1 [$I > 2\sigma(I)$]	0.0260	0.0461	0.0514	0.0384
R_1 (all data)[a]	0.0261	0.0474	0.0521	0.0397
wR_2 (all data)[a]	0.0552	0.1187	0.1427	0.0927
exti coeff	0.010(2)	0.038(10)		
largest diff peak, $e/Å^3$	0.225	0.273	0.304	0.271
largest diff hole, $e/Å^3$	−0.203	−0.420	−0.204	−0.251

[a] $R_1 = \Sigma||F_o| - |F_c||/\Sigma|F_o|$; $wR_2 = \{\Sigma[w(F_o^2 - F_c^2)^2]/\Sigma[w(F_o^2)^2]\}^{1/2}$; $w = 1/[\sigma^2(F_o^2) + (aP)^2 + bP]$, where $P = (F_o^2 + 2F_c^2)/3$.

TABLE 2: Molecular Dimensions (Angstroms and Degrees) and Intermolecular Distances (Angstroms) for 11DCE[a]

	0.1 MPa/100.0(1) K	0.1 MPa/160.0(1) K	0.59(5) GPa/295(2) K	1.51(5) GPa/295(2) K
Cl1−C1	1.7903(14)	1.789(2)	1.787(5)	1.782(3)
C1−C2	1.500(3)	1.493(5)	1.504(13)	1.501(8)
C1−H11	0.98(3)	0.95(4)	0.87(4)	0.97(4)
C2−H21	0.952(19)	0.94(3)	0.84(3)	0.97(3)
C2−H22	0.945(16)	0.93(3)	0.84(3)	0.97(3)
Cl1−C1−$Cl1^{i}$	108.34(12)	108.37(17)	108.0(5)	108.1(3)
Cl1−C1−C2	111.01(11)	110.72(14)	111.0(3)	110.8(2)
Cl1−C1−H11	106.3(8)	105.4(11)	110(2)	104.8(19)
C1−C2−H21	107.5(18)	107(3)	100(4)	103(4)
C1−C2−H22	110.1(12)	107.3(18)	109(2)	106(2)
C2−C1−H11	113.6(15)	116(2)	108(4)	117(4)
H21−C2−H22	109.1(12)	111.3(15)	113(2)	113.3(18)
Cl1−C1−C2−H21	−60.28(11)	−60.12(14)	−60.1(3)	−60.0(2)
Cl1−C1−C2−H22	58.4(9)	59.3(10)	58.1(13)	59.3(11)
Cl1−C1−C2−$H22^{i}$	−179.0(9)	−179.6(10)	−178.3(13)	−179.3(11)
$Cl1^{i}$−C1−C2−H21	60.28(11)	60.12(14)	60.1(3)	60.0(2)
$Cl1^{i}$−C1−C2−H22	179.0(9)	179.6(10)	178.3(13)	179.3(11)
$Cl1^{i}$−C1−C2−$H22^{i}$	−58.4(9)	−59.3(10)	−58.1(13)	−59.3(11)
H11−C1−C2−H21	180.000(3)	180.000(4)	180.000(7)	180.000(7)
H11−C1−C2−H22	−61.3(9)	−60.5(10)	−61.8(13)	−60.7(11)
H11−C1−C2−$H22^{i}$	61.3(9)	60.5(10)	61.8(13)	60.7(11)
Cl1···$Cl1^{ii}$	3.6904(9)	3.7453(14)	3.5910(36)	3.5218(20)
Cl1···$H22^{iii}$	3.08(1)	3.15(2)	3.03(2)	2.91(3)

[a] Symmetry codes: (i) x, $^3/_2 - y$, z; (ii) $2 - x$, $1 - y$, $-z$; (iii) $^3/_2 - x$, $1 - y$, $-^1/_2 + z$.

spectroscopy[47] and are similar to those observed for other analogous compounds.[11,48−50] The structures at 160 and 100 K are very similar: interatomic distances, valence angles, and torsion angles agree within 3 estimated standard deviations (esds) at both studied temperatures, while a systematic contraction of intermolecular contacts has been observed, the largest for the Cl1···$Cl1^{ii}$ distance of 0.0549(17) Å (Table 2).

Similarly, the pressure-induced changes in the intramolecular bonds and angles between 0.59 and 1.51 GPa do not exceed 3 esds, but they are clearly seen in the intermolecular Cl···Cl distances between 11DCE molecules of neighboring *ac* planes (Table 2, Figures 2 and 3).

Surprisingly, only at pressure approaching 1.5 GPa do the Cl···Cl and Cl···H intermolecular contacts became commensurate with the sum of the van der Waals radii of Cl and H.[51−53] Halogenated compounds without Cl···Cl interactions in their crystal structures have already been observed, for example, the ambient- and high-pressure phases of chlorotrimethylsilane.[54] The H···H contacts in 11DCE are the longest when related to the sum of the van der Waals radii: the shortest H···H distance at 1.51 GPa is ca. 0.6 Å longer than the sum of the van der Waals radii of 2.4 Å (Table 2, Figure 3).

However the most striking feature of the ambient-pressure 11DCE crystal is that there are no close contacts of any kind in the structure. It is apparent that, with all intermolecular distances longer, on average, by 0.3−0.4 Å than the sums of van der Waals radii, the energy of the intermolecular interactions is low. It is characteristic that by lowering the temperature from 160

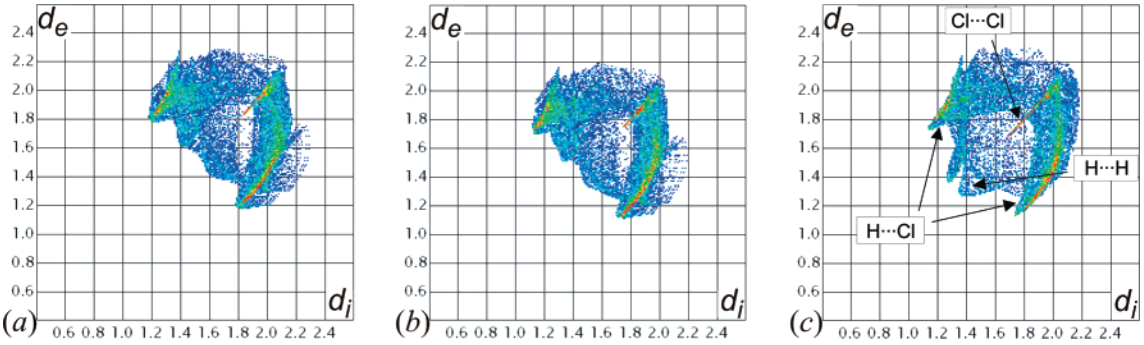

Figure 5. Two-dimensional fingerprint plots for the structures of 11DCE at (a) 0.1 MPa/100 K and (b) at 1.51 GPa/295 K and (c) for the structure of 12DCE at 0.1 MPa/110 K. The fingerprint plot regions corresponding to different interaction types have been indicated. The program CrystalExplorer[40,41] was used for preparing these drawings.

TABLE 3: Comparison of Selected Structural and Thermodynamic Parameters for Ambient Pressure 11DCE at 100 K and 12DCE at 110 K

	11DCE	12DCE
melting point, K	176.19	237.6
enthalpy of melting, J·mol^{-1}	7870	8837
entropy of melting, J·K^{-1}·mol^{-1}	44.77	37.25
boiling point, K	330.5	356.6
density, g·cm^{-3}	1.552	1.601
crystal site symmetry	*m*	$\bar{1}$
space group	*Pnma*	$P2_1/c$
molecular coordination number	14	14
packing coefficient	0.70	0.72
Kitajgorodskij's category	limitingly close-packed	closest-packed

to 100 K the intermolecular distances contracted on average by about 0.07 Å and remain considerably longer than the sums of van der Waals radii. The van der Waals spheres do not touch even at 0.59 GPa, and only pressure of ca. 1.5 GPa brings them in contact (compare Figures 3 and 4). The structure at 160 K/0.1 MPa is ca. 15% less dense than that one at 295 K/1.51 GPa (Table 1). This is clearly reflected in the intermolecular Cl1···Cl1^{ii} and Cl1···H22^{iii} distances squeezed to 95.9 and 96.2% between the 160 K/0.1 MPa and 295 K/0.59 GPa, respectively, and to 94.0 and 92.4% at 1.51 GPa (Table 2, Figure 3).

3.2. Structural and Thermodynamic Properties of 11- and 12DCE. The structural and thermodynamic parameters of 11DCE at 100 K and 12DCE at 110 K[48] have been compared in Table 3.

The intermolecular distances for 11- and 12DCE can be compared using the two-dimensional diagrams-fingerprint plots (Figure 5).[40,41] Lowering temperature and increasing pressure decreased the Cl···Cl, Cl···H, and H···H distances and increased density, which hardly affected fingerprint plots of 11DCE (except for slight shifts of d_e and d_i to lower values: parts a and b of Figure 5), but they are clearly different from the fingerprint plot of 12DCE (Figure 5c).

Whereas in 11DCE the molecular symmetry C_s is preserved in crystal (limitingly close-packed Kitajgorodskij's category), in 12DCE the C_{2h} symmetric molecules are located at inversion centers in the monoclinic $P2_1/c$ structure. The 14-fold molecular coordination and a packing coefficient of 0.72[48] are very similar to those calculated for the structure of 11DCE at 100 K (Table 3).

The differences in properties of the two isomers—higher melting and boiling points and higher density of 12DCE than of 11DCE—on the molecular level can be explained by a different-packing efficiency, which in turn depends on the intermolecular interactions and shape of molecules. All of these factors are more favorable for the 12DCE: (i) the electronegative chlorine atoms are located at the opposite methylene carbons and do not compete in withdrawing charges; (ii) owing to the 1,2-distant location the electronic structure of the chlorine atoms do not interfere (in 11DCE the negative rims are very close); (iii) the 1,2-location secures a free access to the chlorine atoms and minimizes sterical hindrances and competition between approaching molecules; and finally (iv) the molecular symmetry (C_{2h}) of 12DCE is favorable because it contains an inversion center (C_i), which is preserved in the crystal and allows 3-dimensional adjustment of molecular surrounding.

From the thermodynamic point of view the melting point $T_m = \Delta H_m/\Delta S_m$ depends on both the enthalpy (ΔH_m) and the entropy (ΔS_m) of melting. The high melting point can be due to either a high enthalpy of melting or low entropy of melting or both simultaneously. ΔH_m is a measure of the amount of energy required to convert the crystal to liquid, whereas ΔS_m is a measure of the increase of randomness or disorder when the molecules are released from the constraints of the crystal into the relative freedom of the liquid. As explained above, there is a significant difference in the enthalpy component between 11- and 12DCE (Table 3). The difference in chemical structure may also have a notable effect on the entropy of melting, which is primarily due to rotational and conformational freedom. In rotationally disordered crystals the entropy of melting is reduced by the rotational disorder already existing in the crystal at the melting point.[2] In 12DCE, owing to the terminal location of the chlorine atoms, the observed rotational disorder of the ethylene moiety does not affect the strongest Cl···Cl interactions, whereas in 11DCE any type of disorder (except for insignificant CH_3 rotations) would interfere with the crystal cohesion forces.

4. Conclusions

We have shown that for 11- and 12DCE the well-known empirical Carnelley's rule—*high molecular symmetry is associated with high melting point*—can be related to the intermolecular interactions in the crystal structure. Also the lower density of 11DCE can be explained by the detailed X-ray crystal structure analysis of the molecular symmetry and intermolecular interactions. The intermolecular forces, in turn, can be explained by the molecular structure, shape, and symmetry. In light of these results, it becomes apparent that generally the van der Waals radii are dependent on the location of the atom in the particular molecule.

The crystal structures of 11DCE and 12DCE illustrate this feature for the van der Waals radii of Cl and H atoms: in 11DCE all Cl···Cl, Cl···H, and H···H distances at 160 K/0.1 MPa are considerably longer than the sums of van der Waals radii. However the close location of the Cl atoms in the 11DCE molecule affects their electronic structure and sterically is

unfavorable for the formation of close contacts; also due to the resultant polarization of the molecule, the close Cl···Cl and H···H contacts are unfavorable electrostatically. Thus the van der Waals radii differ depending on the location of atoms in specific molecules.

Acknowledgment. This material is based upon work partly supported by the Polish Ministry of Science and Information Technology, Grant No. NN204195633.

Supporting Information Available: Crystallographic data in CIF format. This material is available free of charge via the Internet at http://pubs.acs.org.

References and Notes

(1) Allen, G.; Brier, P. N.; Lane, G. *Trans. Faraday Soc.* **1967**, *63*, 824−832.
(2) Brown, R. J. C.; Brown, R. F. C. *J. Chem. Educ.* **2000**, *77*, 724−731.
(3) Sabharwal, R. J.; Huang, Y.; Song, Y. *J. Phys. Chem. B* **2007**, *111*, 7267−7273.
(4) Wei, J. *Ind. Eng. Chem. Res.* **1999**, *38*, 5019−5027.
(5) Zhao, L.; Yalkowsky, S. H. *Ind. Eng. Chem. Res.* **1999**, *38*, 3581−3584.
(6) Thalladi, V. R.; Boese, R.; Weiss, H. C. *J. Am. Chem. Soc.* **2000**, *122*, 1186−1190.
(7) Slovokhotov, Y. L.; Neretin, I. S.; Howard, J. A. K. *New. J. Chem.* **2004**, *28*, 967−979.
(8) Bond, A. D. *Cryst. Eng. Commun.* **2006**, *8*, 333−337.
(9) Godavarthy, S. S.; Robinson, R. L., Jr.; Gasem, K. A. M. *Ind. Eng. Chem. Res.* **2006**, *45*, 5117−5126.
(10) Bujak, M.; Dziubek, K.; Katrusiak, A. *Acta Crystallogr.* **2007**, *B63*, 124−131.
(11) Bujak, M.; Budzianowski, A.; Katrusiak, A. *Z. Kristallogr.* **2004**, *219*, 573−579.
(12) Bujak, M.; Katrusiak, A. *Z. Kristallogr.* **2004**, *219*, 669−674.
(13) Grineva, O. V.; Zorkii, P. M. *Zh. Fiz. Khim.* **1998**, *72*, 714−720.
(14) Grineva, O. V.; Zorkii, P. M. *J. Struct. Chem.* **2001**, *42*, 16−23.
(15) McClellan, A. L.; Nicksic, S. W. *J. Phys. Chem.* **1965**, *69*, 446−449.
(16) Miyajima, G.; Takahashi, K. *J. Phys. Chem.* **1971**, *75*, 331−334.
(17) Daasch, L. W.; Liang, C. Y.; Nielsen, J. R. *J. Chem. Phys.* **1954**, *22*, 1293−1303.
(18) Durig, J. R.; Sloan, A. E.; Witt, J. D. *J. Phys. Chem.* **1972**, *76*, 3591−3597.
(19) McKean, D. C.; Laurie, B. W. *J. Mol. Struct.* **1975**, *27*, 317−328.
(20) de Luis, A.; López, J. C.; Alonso, J. L. *Chem. Phys.* **1999**, *248*, 247−261.
(21) Brier, P. N.; Higgins, J. S.; Bradley, R. H. *Mol. Phys.* **1971**, *21*, 721−744.
(22) Danford, M. D.; Livingston, R. L. *J. Am. Chem. Soc.* **1959**, *81*, 4157−4159.
(23) Mark, J. E.; Sutton, C. *J. Am. Chem. Soc.* **1972**, *94*, 1083−1090.
(24) Lide, D. R. *CRC Handbook of Chemistry and Physics*, 75th ed.; CRC Press Inc.: Boca Raton, FL, 1994.
(25) Amoureux, J. P.; Foulon, M.; Muller, M.; Bee, M. *Acta Crystallogr.* **1986**, *B42*, 78−84.
(26) Vorontsov, I. I.; Almásy, L.; Antipin, M. Yu. *J. Mol. Struct.* **2002**, *610*, 271−276.
(27) Podsiadło, M.; Dziubek, K.; Szafrański, M.; Katrusiak, A. *Acta Crystallogr.* **2006**, *B62*, 1090−1098.
(28) Merrill, L.; Bassett, W. A. *Rev. Sci. Instrum.* **1974**, *45*, 290−294.
(29) Fourme, R. *J. Appl. Cryst.* **1968**, *1*, 23−30.
(30) Vos, W. L.; Finger, L. W.; Hemley, R. J.; Mao, H. *Phys. Rev. Lett.* **1993**, *71*, 3150−3153.
(31) Allan, D. R.; Clark, S. J., Brugmans; M. J. P., Ackland, G. J.; Vos, W. L. *Phys. Rev. B: Condens. Matter Mat. Phys.* **1998**, *58*, R11809−R11812.
(32) Katrusiak, A. *J. Appl. Cryst.* **1999**, *32*, 1021−1023.
(33) Piermarini, G. J.; Block, S.; Barnett, J. D.; Forman, R. A. *J. Appl. Phys.* **1975**, *46*, 2774−2780.
(34) Budzianowski, A.; Katrusiak, A. In *High-Pressure Crystallography*; Katrusiak, A., McMillan, P. F., Eds.; Kluwer Academic Publishers: Dordrecht, The Netherlands, 2004; pp 101−112.
(35) Oxford Diffraction. *CrysAlis CCD, Data collection GUI for CCD and CrysAlis RED CCD data reduction GUI, versions 1.171.24 beta*; Wrocław, Poland, 2004.
(36) Sheldrick, G. M. *SHELXTL*; Siemens Analytical X-ray Instrument Inc.: Madison, WI, 1990.
(37) Katrusiak, A. *REDSHABS*; Adam Mickiewicz University: Poznań, Poland, 2003.
(38) Katrusiak, A. *Z. Kristallogr.* **2004**, *219*, 461−467.
(39) Sheldrick, G. M. *SHELX-97*; University of Göttingen: Göttingen, Germany 1997.
(40) Wolff, S. K.; Grimwood, D. J.; McKinnon, J. J.; Jayatilaka, D.; Spackman, N. A. *CrystalExplorer 2.0 (r 313)*; University of Western Australia: Perth, Australia 2007; http://hirshfeldsurface.net/CrystalExplorer/.
(41) McKinnon, J. J.; Spackman, M. A.; Mitchell, A. S. *Acta Crystallogr.* **2004**, *B60*, 627−668.
(42) Dziubek, K.; Katrusiak, A. *J. Phys. Chem.* **2004**, *B108*, 19089−19092.
(43) *XP*; Siemens Analytical X-ray Instruments Inc.: Madison, Wisconsin, 1990.
(44) Wilson, A. J. C. *Acta Crystallogr.* **1993**, *A49*, 210−212.
(45) Kitajgorodskij, A. I. *Molekularnyje Kristally*; Nauka: Moscow, 1972.
(46) Peresypkina, E. V.; Blatov, V. A. *Acta Crystallogr.* **2000**, *B56*, 501−511.
(47) Sugie, M.; Kato, M.; Matsumura, C.; Takeo, H. *J. Mol. Struct.* **1997**, *413*−414, 487−494.
(48) Boese, R.; Bläser, D.; Haumann, T. *Z. Kristallogr.* **1992**, *198*, 311−312.
(49) Podsiadło, M.; Dziubek, K.; Katrusiak, A. *Acta Crystallogr.* **2005**, *B61*, 595−600.
(50) Podsiadło, M.; Katrusiak, A. *Acta Crystallogr.* **2006**, *B62*, 1071−1077.
(51) Bondi, A. *J. Phys. Chem.* **1964**, *68*, 441−451.
(52) Nyburg, S. C.; Faerman, C. H. *Acta Crystallogr.* **1985**, *B41*, 274−279.
(53) Batsanov, S. S. *Inorg. Mater.* **2001**, *37*, 871−885.
(54) Gajda, R.; Dziubek, K.; Katrusiak, A. *Acta Crystallogr.* **2006**, *B62*, 86−93.